Journal of Molecular Structure, 300 (1993) 313–324
0022-2860/93/\$06.00 © 1993 – Elsevier Science Publishers B.V. All rights reserved

The dipole gradient for isolated C–H stretches
2. Partially deuterated methyl fluoride, methyl chloride and methyl iodide

A.Y. Grupping[a], D.C. McKean[b,1], B.J. van der Veken[a,*]

[a]*Department of Chemistry, Universitair Centrum Antwerpen, Groenenborgerlaan 171, B-2020 Antwerp, Belgium*
[b]*Department of Chemistry, University of Aberdeen, Meston Walk, Old Aberdeen, Aberdeen AB9 2UE, Scotland, UK*

(Received 19 April 1993)

Abstract

The vapour phase infrared contours, at 0.5 cm^{-1} resolution, of the C–H stretch fundamental in CHD_2F, CHD_2Cl and CHD_2I have been simulated using anharmonic rigid asymmetric top calculations. The smallest angle between the C–H bond direction and the dipole gradient that reproduces the experimental contour, obtained by rotating the gradient from the C–H bond towards the bisector of the methyl group, was found to be 15 ± 5° in CHD_2F, 38 ± 2° in CHD_2Cl and 49 ± 3° in CHD_2I. Together with the corresponding value for CHD_2Br, these results are compared with the polarizability of the halogen atom.

Introduction

The characteristic spectroscopic properties of isolated C–H stretches [1] have been successfully exploited in the analysis of conformational problems on a number of occasions [2–5]. In all these cases, the vapour phase infrared contours were predicted from the bond dipole model (BDM) in which it is assumed that the dipole gradient $(\partial\vec{\mu}/\partial Q)_0$ for the stretching of the isolated C–H bond is oriented along the C–H bond. Recently, however, the analysis of the infrared contour of the C–H stretch in CHD_2Br [6] has shown that the direction of the dipole gradient for this vibration differs considerably from the C–H bond orientation. This conclusion was found to be in agreement with predictions from the atomic polar tensor analysis of the methyl halides by Newton and Person [7]. Similarly, from this latter analysis of the C–H stretch in CHD_2F, CHD_2Cl and CHD_2I, it can be predicted that the BDM will fail. Therefore, in order to get a better understanding of the factors that influence the orientation of the dipole gradient, the vapour phase infrared contours of the C–H stretch in these partially deuterated methyl halides have been investigated, and the results are reported below.

The molecules studied here have C_S symmetry and have their C–H bond in the plane of symmetry. This plane contains the *a* and *c* axes, and consequently the C–H stretch fundamental must show an *A*/*C* hybrid contour. The direction of the dipole gradient in the principal axes system then is determined by the direction cosines $\cos\alpha$ and $\cos\gamma$. Because the sum of the squares of the direction

---

[*] Corresponding author.
[1] Present address: Department of Chemistry, University of Edinburgh, West Mains Road, Edinburgh, EH9 2JJ, Scotland, UK.

cosines must be equal to unity, the hybrid contours simulated here are functions of a single parameter only. We identify this parameter with the gradient angle ω, defined as the angle between the direction of the dipole gradient and the C–H bond orientation. Positive values of this angle are obtained by rotating the gradient from the C–H bond towards the bisector of the methyl group, i.e. away from the carbon–halogen bond.

In the expression for a hybrid contour only squares of direction cosines appear. In the present study this implies that two values of the gradient angle lead to the same hybrid. In view of the BDM, the smallest of the two values appears physically to be the more likely, and will therefore be used here. This choice at least ensures that the deviations from the BDM shown by the C–H stretch in the partially deuterated methyl halides can be correctly appreciated.

Experimental

Partially deuterated methyl chloride, CHD_2Cl, was prepared as described previously [8]. CHD_2I was formed by adding P and I_2 to the partially deuterated alcohol CHD_2OH (MSD Isotopes, MD-758). Methyl fluoride-d_2, CHD_2F, was synthesized by the direct halogen exchange between CHD_2I and AgF_2. The reaction products were purified using a low-temperature and low-pressure fractionating column. Careful analysis of the infrared spectra of the purified compounds showed that no traces of the CH_2DX and CH_3X derivatives could be detected, i.e. no scrambling of the hydrogen and deuterium had occurred during the reactions.

The infrared spectra were recorded on a Bruker 113v Fourier transform spectrometer equipped with a Ge/KBr beamsplitter and a Globar source. For CHD_2Cl, 0.1 cm^{-1} and 0.5 cm^{-1} resolution spectra were measured at vapour pressures of 48 mbar and 46 mbar, respectively. For CHD_2I, these pressures were equal to 70 mbar and 90 mbar, respectively. A 0.5 cm^{-1} resolution spectrum of the vapour phase CHD_2F was measured at a pressure of 4 mbar. A 30 cm gas cell fitted with KBr windows and connected to a vacuum manifold was used to contain the vapours. Happ–Genzel apodised interferograms from 500 scans were Fourier transformed. All infrared spectra were recorded using a broad-band MCT detector.

Rigid asymmetric top calculations were performed to a maximum J value equal to 80 for CHD_2F and CHD_2Cl and 90 for CHD_2I. At these values the contours were found to be sufficiently converged. The convolution of the calculated intensities was performed with the Happ–Genzel instrumental lineshape function, analogous to the calculations for the partially deuterated methyl bromide [6].

At the resolution used, no differences could be seen between the contours calculated for the different isotopes of the halogen atoms. Therefore, final calculations of the pure-type transitions were performed for hypothetical molecules in which the halogen was assigned the isotopically averaged atomic mass.

Model calculations showed that centrifugal distortion at this level of resolution introduces minor effects only in the regions far from the band centre. Because we were interested in the more central region of the absorption band, centrifugal distortion was neglected in the subsequent study.

Discussion

In Fig. 1, the projection of CHD_2Cl in the

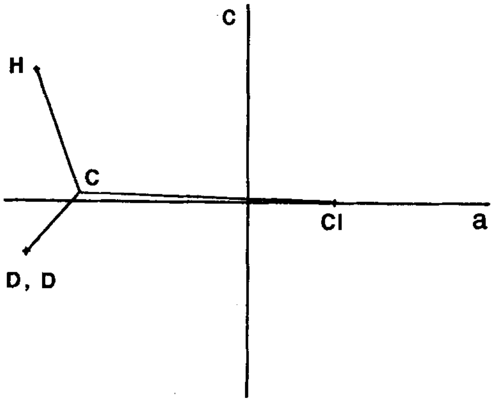

Fig. 1. Projection of CHD_2Cl in the a,c-plane of the principal axis system.

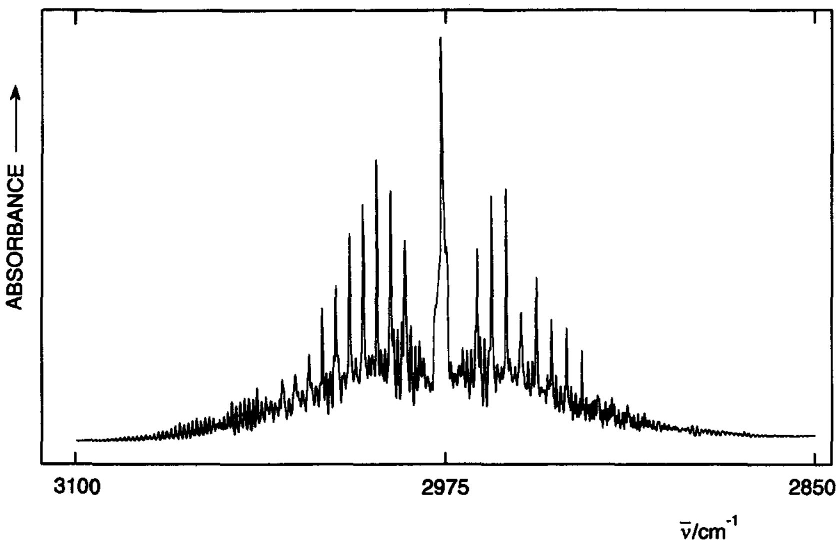

Fig. 2. The vapour phase infrared spectrum of CHD_2F in the C–H stretch region, recorded at 0.5 cm^{-1} resolution.

a,*c*-plane of the principal axes system is shown. As could be anticipated, the *a* axis is very close to the C–Cl bond. The latter, in a symmetrically substituted derivative such as CH_3Cl, is the symmetry axis of the symmetric top. As a consequence, the partially deuterated molecule is a near symmetric top. Therefore, just as in CHD_2Br [6], the pure type-A transition will show a pseudo-parallel contour, while the type-C transition will give rise to a pseudo-perpendicular contour.

In Figs. 2–4 the experimental vapour phase infrared contours for the C–H stretch in CHD_2F, CHD_2Cl and CHD_2I, recorded at 0.5 cm^{-1} resolution, are given. The type-*C* contribution to the experimental contours is characterized by sharp, equidistant *Q*-type fine structure lines in the *P*- and *R*-branches, while the type-*A* contribution is responsible for most of the continuous intensity in *P* and *R*. Because the asymmetry in the molecules is caused by the deuterium atoms and not by

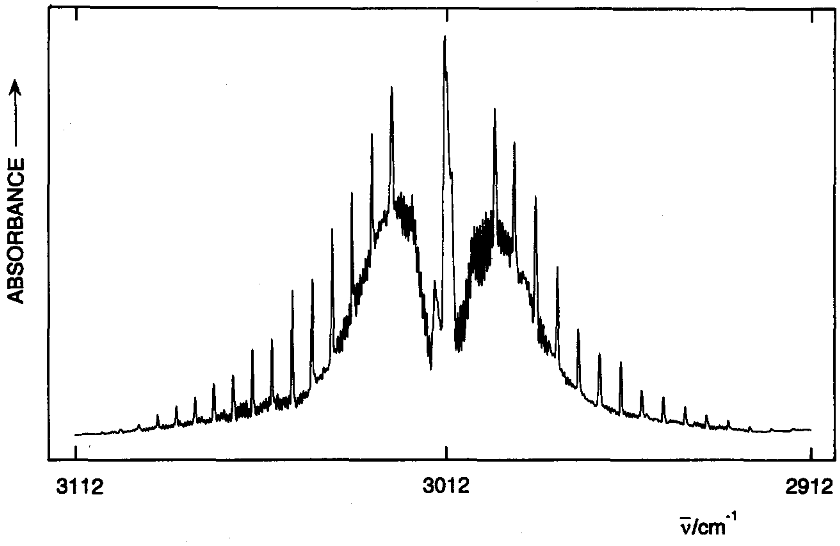

Fig. 3. The vapour phase infrared spectrum of CHD_2Cl in the C–H stretch region, recorded at 0.5 cm^{-1} resolution.

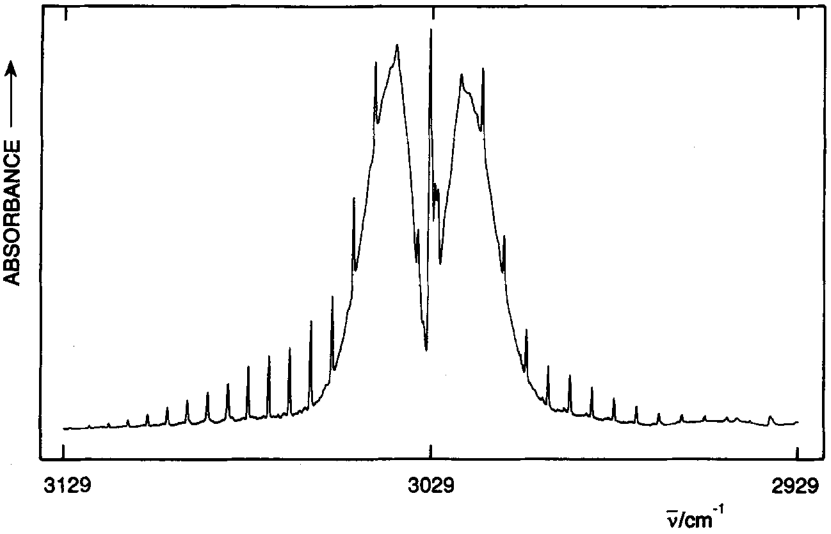

Fig. 4. The vapour phase infrared spectrum of CHD_2I in the C–H stretch region, recorded at 0.5 cm^{-1} resolution.

the halogen atom, both CHD_2F and CHD_2I have an orientation in their principal axes very similar to the one shown in Fig. 1 for CHD_2Cl. Nevertheless, as is clear from Figs. 2–4, from CHD_2F to CHD_2I there is a systematic decrease in the relative intensities of the type-*C* *Q*-subbands with respect to the intensity of the continuous background in *P* and *R*. This decrease therefore suggests that in this series the orientation of the dipole gradient for the C–H stretch changes considerably. It is the aim of the discussion below to quantify these observations.

Methyl fluoride-d$_2$

Equilibrium rotational constants for partially deuterated methyl fluoride were derived from the geometry described by Duncan [9]. The data used, together with the equilibrium rotational constants, are gathered in Table 1. It is clear from the asymmetry of the contour in Fig. 2 that for a quantitative simulation of the experimental contour, anharmonic rotational constants are needed. In the least squares optimization process used to obtain such anharmonic constants, as described for CHD_2Br [6], assignments of a number of transitions must be made. This proved to be difficult for CHD_2F, because *K* fine structure is present in the pseudo-parallel lines. Therefore, no optimization of anharmonic rotational constants was attempted. Both the studies of CHD_2Br [6] and of CHD_2Cl and CHD_2I (vide infra) suggest that, at the level of approximation used, the anharmonic rotational constants based on an ab initio cubic force field are quite satisfactory. Therefore, for CHD_2F, rotational constants for the vibrational ground and excited states were calculated from

$$B_v = B_e - \sum_r \alpha_r^B (v_r + d_k/2)$$

in which the ab initio values for α_v^B, calculated by Thiel and Schneider [10], were used. The rotational constants obtained in this way are given in Table 2.

Table 1
Equilibrium geometrical data and rotational constants[a]

	CHD_2F	CHD_2Cl	CHD_2I
$r_e(CH) = r_e(CD)$	1.090	1.0854	1.084
$r_e(C{-}X)$	1.382	1.7760	2.132
$\alpha_e(H{-}C{-}H)$	110.5	110.35	111.2
A_e	3.183	3.213	3.185
B_e	0.7550	0.3906	0.2183
C_e	0.7174	0.3805	0.2151

[a] Bond lengths in Ångströms, bond angles in degrees, rotational constants in cm^{-1}.

Table 2
Anharmonic rotational constants[a] for CHD_2F

A'	3.147	A''	3.132
B'	0.7492	B''	0.7495
C'	0.7114	C''	0.7117

[a] All rotational constants are given in cm^{-1}.

As is clear from Fig. 2, it would be extremely difficult to reliably delimit the continuous background in the P- and R-branches. Consequently, it is very difficult to quantify the type-A contribution to the experimental hybrid. The abstraction of the hybrid content is further hampered by the irregularities of the type-C Q-subbands in the P-branch. Therefore, for CHD_2F the gradient angle ω could not be obtained by the procedure applied for CHD_2Br [6]. Instead, a qualitative value for the gradient angle was obtained from a visual comparison of calculated contours with the experimental one. The best agreement was obtained for ω equal to 15°. Although this method is not very precise, it was clear that the hybrids calculated for $\omega = 10°$ and for $\omega = 20°$ agreed less well. Therefore, the gradient angle can be set at $15 \pm 5°$. The hybrid calculated for this orientation is compared with the experimental contour in Fig. 5.

Methyl chloride-d_2

The rotational fine structure observed for methyl chloride-d_2 is more regular than the one observed for CHD_2F, and hence a more detailed study was possible. Equilibrium rotational constants were calculated from the equilibrium geometry described by Jensen et al. [11]. These data are given in Table 1. The frequencies of a number of ^PQ_n and ^RQ_n band maxima were accurately measured in a $0.1\,cm^{-1}$ resolution spectrum. Based on statistical theory, these maxima had to be assigned to transitions between states with J equal to 16. Also in the $0.1\,cm^{-1}$ resolution spectrum, a number of $(B+C)$-type fine structure bands from the type-A contribution were accurately measured. These were assigned to transitions between levels having the K_a value equal to one. Using these frequencies and their assignments, rotational constants for the ground and excited vibrational states were adjusted from the equilibrium values by a diagnostic least squares procedure [12]. The resulting anharmonic rotational constants are collected in Table 3.

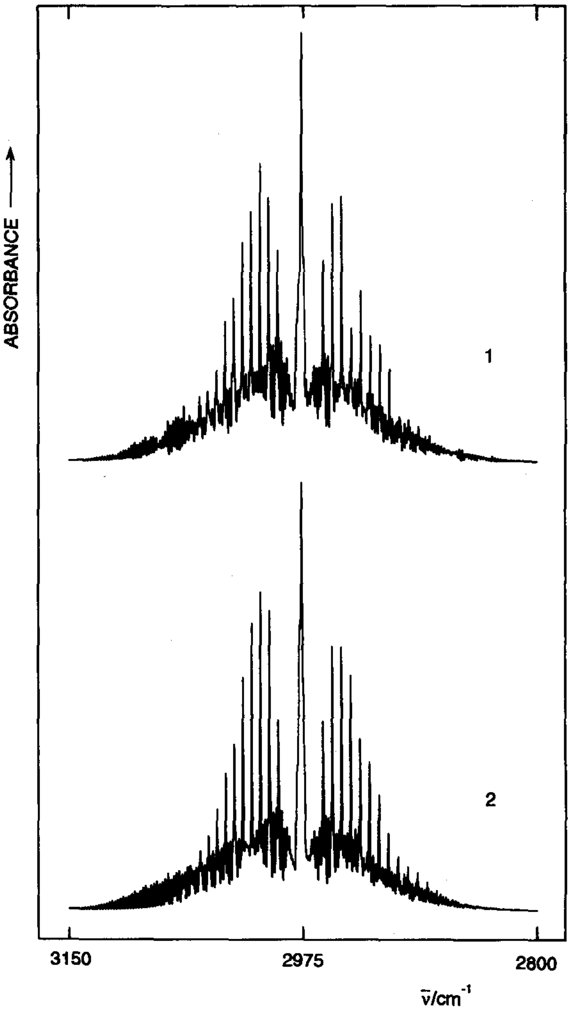

Fig. 5. The vapour phase infrared contour of the C–H stretch in CHD_2F at $0.5\,cm^{-1}$ resolution: (1) experimental contour; (2) simulation for a gradient angle of 15°.

For CHD_2Cl, the values of α_r^B have also been calculated by Thiel and Schneider [10] using an ab initio cubic force field. These values, together with the equilibrium rotational constants, were used to calculate a second set of anharmonic

Table 3
Anharmonic rotational constants[a] for CHD_2Cl

	I[b]	II[c]	III[d]
A'	3.176(2)	3.182	3.193
A''	3.160(2)	3.168	3.151
B'	0.3899(8)	0.3879	0.3902
B''	0.3913(8)	0.3881	0.3891
C'	0.3809(7)	0.3777	0.3803
C''	0.3800(7)	0.3779	0.3801

[a] All rotational constants are given in cm^{-1}.

[b] Obtained from diagnostic least squares calculations; the uncertainties on the last digit are given in brackets.

[c] Calculated from ab initio α_rs.

[d] Calculated from Morse potential.

rotational constants. The latter have also been collected in Table 3.

Finally, anharmonic rotational constants were obtained from the Morse model, in which the C–H stretch is represented by a Morse oscillator [13]. The fundamental and the first three overtone frequencies, determined by Baggott et al. [14] were used in the least squares calculation of the parameters of the Morse potential. These parameters are given in Table 4. Using the Morse functions for the ground and first excited states of the C–H stretch, vibrationally averaged rotational constants were calculated. These anharmonic rotational constants are given in Table 3.

Pure type-A and type-C transitions were calculated at $0.5\,cm^{-1}$ resolution, using each of the three sets of rotational constants from Table 3. As an example, in Fig. 6 the pure type-A transitions are compared. It can be seen that the least squares optimized rotational constants and the ab initio rotational constants lead to similar contours, while the Morse model predicts a much more perturbed contour. The latter, for instance, shows a much broader Q-branch. Experimentally, however, as can be seen from Fig. 3, a rather narrow

Table 4
Observed C–H stretch frequencies and Morse potential parameters for CHD_2Cl

Transition	Observed frequency (cm^{-1})
$1 \leftarrow 0$	3012.22
$2 \leftarrow 0$	5898.47
$3 \leftarrow 0$	8670.59
$4 \leftarrow 0$	11323.13
Morse parameters	
a	1.8142 Å
D	$41017\,cm^{-1}$

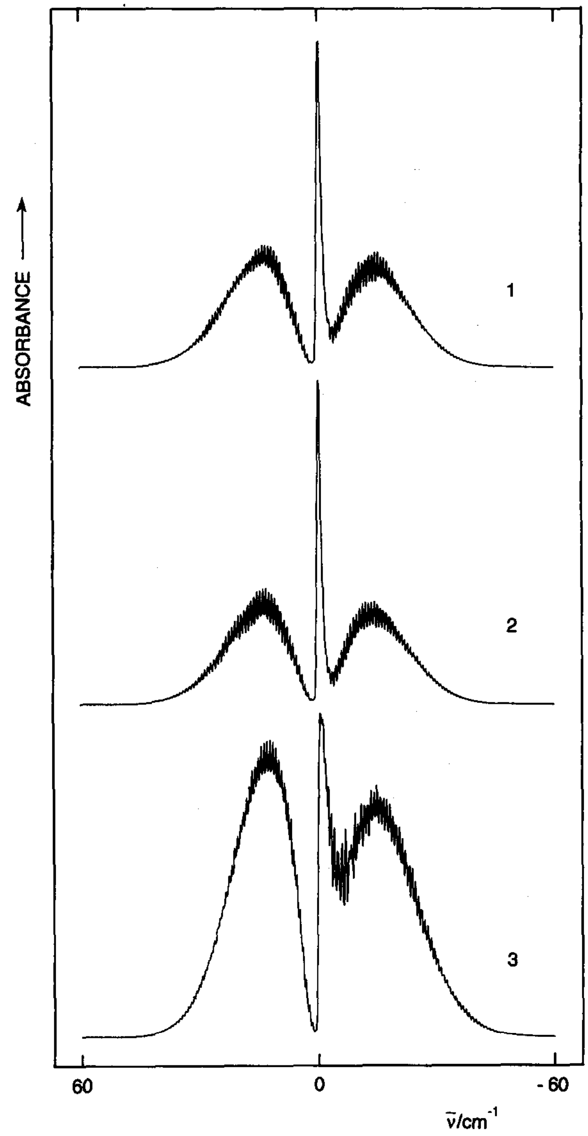

Fig. 6. Pure type-A contours for different sets of anharmonic rotational constants of CHD_2Cl: (1) calculation using least squares optimized rotational constants; (2) calculation using ab initio α_r^B constants; (3) calculation using Morse oscillator model.

central Q-branch is observed. This immediately shows that the Morse model overestimates the anharmonic influences. A similar observation was made for CHD_2Br [6]. As a consequence, no further calculations were made from the Morse anharmonic rotational constants.

The orientation of the dipole gradient, expressed as the gradient angle ω, was obtained as described previously [6]. In short, a series of hybrids were calculated for an increasing angle ω. For each hybrid, the integrated intensity of the continuous background of the P- and R-branches and of a selected number of sufficiently intense ^PQ_n and ^RQ_n bands were determined. For CHD_2Cl, the continuous background was integrated between 3132.2 and 3014.7 cm^{-1} for the R-branch, and between 3009.7 and 2892.2 cm^{-1} for the P-branch. The Q-subbands considered were $^RQ_5$ through $^RQ_{12}$ and $^PQ_5$ through $^PQ_{14}$. From these, the ratios r of the intensity of each ^PQ_n and ^RQ_n to the intensity of the continuous background were calculated. For each ^PQ_n- and ^RQ_n-subband, the r values for the different theoretical hybrids were plotted against the value of the gradient angle ω. Through these points, a second-order polynomial was fitted. By measuring the corresponding ratio r in the experimental spectrum, the polynomial could be interpolated to produce a value for ω. The uncertainties on the interpolated ω values were estimated as before [6]. In Fig. 7, the interpolated values of ω, obtained using hybrids from the least squares optimized rotational constants are shown. The abscissa values specify the value of n for the ^RQ_n- or ^PQ_n-band used. The numerical values of ω used to construct Fig. 7 are given in Table 5. As could be expected from the resemblance of the two sets of rotational constants, the ω values obtained using ab initio anharmonic constants were found to be similar. Therefore, in the subsequent analysis only one set of values was used. For the R-branch, the mean value of ω is 36 ± 3°, while the corresponding value for the P-branch was calculated to be 40 ± 3°. The difference between these two values is presumably partly caused by the neglect of centrifugal distortion. Also, because anharmonicity tends to redistribute P- and R-branch intensities, shortcomings in the anharmonic models used to calculate the theoretical hybrids will contribute to the difference. The final value for ω was calculated as the weighted average of all the values in Table 5.

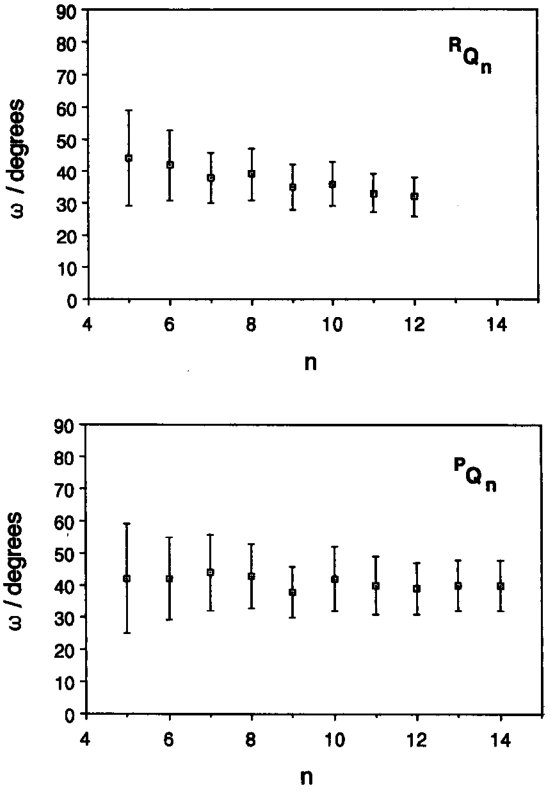

Fig. 7. The experimental values for the gradient angles ω obtained from the C–H stretch contour of CHD_2Cl.

Table 5
Gradient angles for CHD_2Cl

Subband	Angle (deg)	Subband	Angle (deg)
$^RQ_5$	44 ± 15	$^PQ_5$	42 ± 17
$^RQ_6$	42 ± 11	$^PQ_6$	42 ± 13
$^RQ_7$	38 ± 8	$^PQ_7$	44 ± 12
$^RQ_8$	39 ± 8	$^PQ_8$	43 ± 10
$^RQ_9$	35 ± 7	$^PQ_9$	38 ± 8
$^RQ_{10}$	36 ± 7	$^PQ_{10}$	42 ± 10
$^RQ_{11}$	33 ± 6	$^PQ_{11}$	40 ± 9
$^RQ_{12}$	32 ± 6	$^PQ_{12}$	39 ± 8
		$^PQ_{13}$	40 ± 8
		$^PQ_{14}$	40 ± 8
Average	36 ± 3	Average	40 ± 3

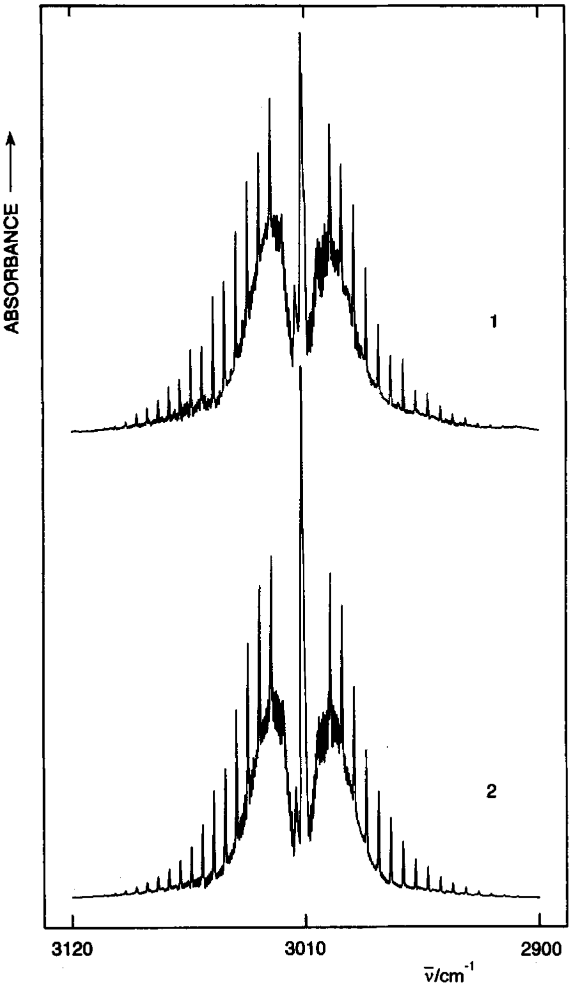

Fig. 8. The vapour phase infrared contour of the C–H stretch in CHD_2Cl at 0.5 cm^{-1} resolution: (1) experimental contour; (2) simulation with a gradient angle of 38°, using least squares optimized anharmonic rotational constants.

This value is equal to 38 ± 2°. The hybrid calculated for this angle between the dipole gradient and the C–H bond is compared with the experimental contour in Fig. 8.

An independent value for ω can be obtained from atomic polar tensor theory. As described by Person and Newton [15], the matrix $\boldsymbol{P}_x$ of atomic polar tensors can be transformed in a matrix $\boldsymbol{P}_Q$ containing cartesian components of the dipole gradients $(\partial\vec{\mu}/\partial Q)_0$ by the following relation:

$$\boldsymbol{P}_Q = \boldsymbol{P}_x \boldsymbol{M}^{-1/2} \boldsymbol{C} \boldsymbol{U}^{\mathrm{t}} \boldsymbol{L}$$

Table 6
Tensor elements[a] of P_Q corresponding to the C–H stretch

	FF 1[b]	FF 2[c]
x	−0.293	−0.293
y	0.000	0.000
z	−0.382	−0.375

[a] The tensor elements are given in D Å^{-1} u$^{-1/2}$.
[b] Force field of ref. 14.
[c] Force field of ref. 15.

In this equation, $\boldsymbol{M}$ is the diagonal matrix of atomic masses, $\boldsymbol{C}$ is the transformation matrix from internal coordinates R to mass weighted cartesian coordinates q ($q = CR$), $\boldsymbol{U}^{\mathrm{t}}$ is the transpose of the transformation matrix from internal to symmetry coordinates S ($S = UR$), and $\boldsymbol{L}$ is the eigenvector matrix in symmetry coordinates ($S = LQ$).

The atomic polar tensors for methyl chloride are reported by Ilieva et al. [16]. These data were transformed to the matrix $\boldsymbol{P}_Q$ using an $\boldsymbol{L}$ matrix which was obtained from a force field of methyl chloride calculated by Duncan [17]. The part of $\boldsymbol{P}_Q$ referring to the C–H stretch normal coordinate is given in Table 6. These numbers define the position of the dipole gradient in the cartesian axes system, with the z axis through the C–Cl bond directed away from the chlorine, and the x axis through the carbon atom in the symmetry plane of the molecule and with the unique hydrogen atom on the positive side. From these components, a value of 34° was finally derived for the angle between the C–H bond and the C–H stretch dipole gradient in CHD_2Cl. In order to test the dependence of this result on the force field applied in the transformation, the same calculations were performed using a different force field for methyl chloride, reported by Schneider and Thiel [18]. The elements of the $\boldsymbol{P}_Q$ matrix obtained with this force field are given in the second column of Table 6. From these, a value of 34° was again calculated for the angle between the dipole gradient and the C–H bond.

Taking into account the probability that the atomic polar tensor value for ω will also show some uncertainty, depending as it does on the uncertain distribution of intensity between the partly overlapping parallel and perpendicular bands in the C–H stretching region, and on assumptions about the Fermi resonances, it may be concluded that there is satisfactory agreement between the values of ω obtained from both methods.

Methyl iodide-d$_2$

Finally, the isolated C–H stretch contour of CHD_2I was also analyzed. Equilibrium rotational constants for this molecule were calculated from the geometrical data reported by Harmony et al. [19]. The structural data, together with the equilibrium rotational constants, are given in Table 1. Again, the experimental contour, shown in Fig. 4, suggests anharmonic rotational constants must be used. Because both for CHD_2Br [6] and CHD_2Cl the Morse model leads to poor simulations, for CHD_2I no attempts were made to obtain anharmonic rotational constants from the Morse approximation. Anharmonic rotational constants were obtained by the least squares fit of rotational fine structure obtained at 0.1 cm^{-1} resolution, and from the ab initio α_r^B values reported by Thiel and Schneider [10] for CHD_2I. For the least squares optimization, the ${}^PQ_n$ and ${}^RQ_n$ band maxima were characterized by a J value of 21, while the K_a value for the type-A fine structure was equal to one or two. The sets of rotational constants obtained by both methods are given in Table 7. Again, as for the other partially deuterated methyl halides, the differences between the constants for the excited state and those of the ground state for both methods are very similar, with the largest difference occurring in the rotational constant A.

Values of ω were obtained from the experimental contour by the procedure described above. Both for the calculated hybrids and for the experimental contour, the continuous background was integrated between 3129.7 and 3030.2 cm^{-1} for the R-branch, and between 3027.2 and 2929.7 cm^{-1} for the P-branch. The Q-subbands used were ${}^RQ_3$ through ${}^RQ_{13}$ and ${}^PQ_4$ through ${}^PQ_{11}$. Also for CHD_2I, no distinction could be made between the $r(\omega)$ relations obtained from the hybrids calculated from the least squares optimized rotational constants and those calculated from the ab initio anharmonic constants. Therefore, in the subsequent analysis only one set of relations was used. The angles ω obtained are collected in Table 8, and are shown graphically in Fig. 9. The average value of ω obtained for the R-branch is 48 ± 3°, and the average value for the P-branch is 54 ± 5°.

The difference between the values for the R- and P-branches, in comparison to CHD_2Br and CHD_2Cl, is somewhat bigger than expected. Apart from the contributions cited above for CHD_2Cl, for CHD_2I a third source will contribute to this difference. In the experimental spectrum, an

Table 7
Anharmonic rotational constants[a] for CHD_2I

	I[b]	II[c]
A'	3.152(2)	3.159
A''	3.137(2)	3.146
B'	0.2164(7)	0.2170
B''	0.2165(7)	0.2171
C'	0.2160(7)	0.2138
C''	0.2156(7)	0.2139

[a] All rotational constants are given in cm^{-1}.
[b] Obtained from diagnostic least squares calculations; the uncertainties on the last digit are given in brackets.
[c] Calculated from the ab initio α_rs.

Table 8
Gradient angles for CHD_2I

Subband	Angle (deg)	Subband	Angle (deg)
${}^RQ_3$	53 ± 25	${}^PQ_4$	56 ± 32
${}^RQ_4$	52 ± 14	${}^PQ_5$	55 ± 19
${}^RQ_5$	50 ± 11	${}^PQ_6$	55 ± 15
${}^RQ_6$	50 ± 11	${}^PQ_7$	53 ± 13
${}^RQ_7$	49 ± 10	${}^PQ_8$	53 ± 13
${}^RQ_8$	48 ± 9	${}^PQ_9$	53 ± 13
${}^RQ_9$	49 ± 10	${}^PQ_{10}$	54 ± 14
${}^RQ_{10}$	48 ± 9	${}^PQ_{11}$	55 ± 14
${}^RQ_{11}$	46 ± 8		
${}^RQ_{12}$	46 ± 8		
${}^RQ_{13}$	46 ± 8		
Average	48 ± 3	Average	54 ± 5

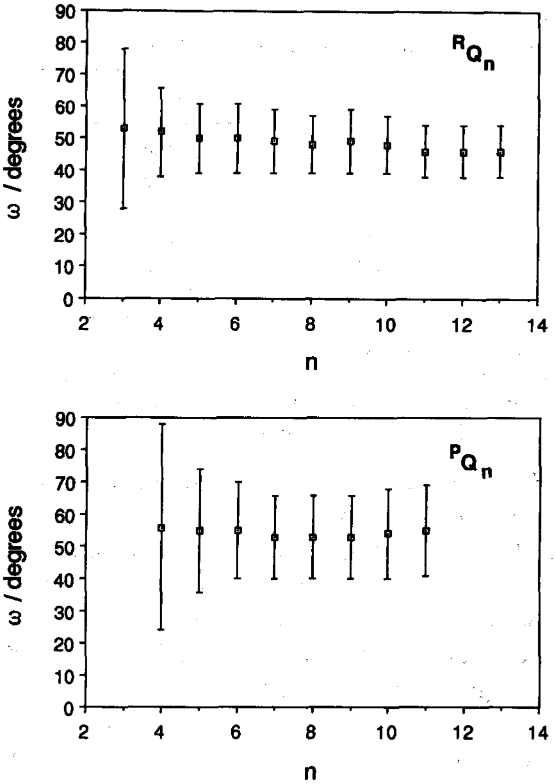

Fig. 9. The experimental values for the gradient angles ω obtained from the C–H stretch contour of CHDI.

unidentified weak absorption is present in the region of the P-branch, with a band centre of approximately 2937 $\mathrm{cm^{-1}}$. In spite of attempts to take account of this disturbance, the integrated intensity of the continuous background of the P-branch presumably is somewhat overestimated. This causes the r values for the ^PQ_n-branches to be too small, and consequently the corresponding ω values are somewhat too large. The final value of ω, the angle between the dipole gradient and the C–H bond, was obtained as the mean of the values in Table 8, and is equal to 49 ± 3°. The hybrid for this direction of the gradient, calculated from the ab initio anharmonic rotational constants, is compared to the experimental contour in Fig. 10.

Conclusion

Using vapour phase infrared band contour simulation, it was shown that the orientation of the dipole gradient for the isolated C–H stretch vibration in all partially deuterated methyl halides differs considerably from the respective C–H bond directions. Moreover, an evolution in the results was ascertained, as shown in Table 9.

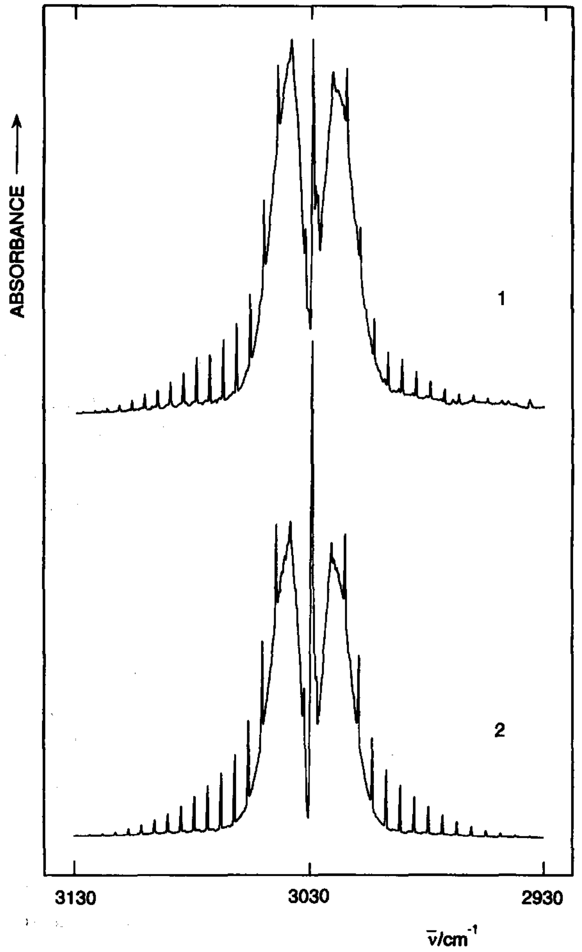

Fig. 10. The vapour phase infrared contour of the C–H stretch in CHD_2I at 0.5 $\mathrm{cm^{-1}}$ resolution: (1) experimental contour; (2) simulation with a gradient angle of 49°, using ab initio anharmonic rotational constants.

The orientation of the dipole gradient is determined by motions of charges and by charge fluxes in the molecule. For the C–H stretch in the present molecules, a distinction can be made between the phenomena occurring in the C–H bond, and the phenomena occurring in the neighbourhood of this bond, generated as a result of the displacements of both atoms, C and H, along the bond direction. If

Table 9
The gradient angle ω for the C–H stretch in all partially deuterated CHD_2X compounds and the polarizability α for HX molecules

X	ω (deg)	$\alpha(\times 10^{-25}\,cm^3)$
F	15 ± 5	8.0
Cl	38 ± 2	26.3
Br	44 ± 2	36.1
I	49 ± 3	54.5

only the first factor is of some importance, the dipole gradient should lie along the C–H bond so that ω is 0°. The charge fluxes occurring in the rest of the molecule cause the angle ω to differ from zero. The evolution of the value of ω in the different methyl halides suggests that the effect must be attributed to a property of the halogen atom. The obvious choice for this property is the polarizability of the halogen atom. As a measure of this, the polarizability of the corresponding HX compounds, taken from ref. 20, are given in Table 9.

In Fig. 11, a plot of ω versus these polarizabilities is shown. It can be seen that ω is not linearly related to the polarizability. However, this is not really expected, as can be seen from the following model. The charge fluxes caused by the stretching of the C–H bond in the rest of the molecule can be represented as a dipole gradient component along the C–X bond. The dipole gradient $(\partial\vec{\mu}/\partial Q)_0$ for the C–H stretching is then the vector sum of this component with the component along the C–H bond, which is caused by the motion and flux of charge in the C–H bond. When the component along the C–X bond is primarily due to charge fluxes in the halogen atom, its length must be expected to vary linearly with the polarizability of the atom X. However, it is clear that, even should the component along the C–H bond be constant, the angle ω in this case will not be a linear function of the polarizability of the halogen atom. Moreover, the qualitative behaviour of the intensity of νCH in the present series of molecules suggests that the gradient component along the C–H bond is not constant. With the knowledge of ω and of the length of $(\partial\vec{\mu}/\partial Q)_0$, as obtained from the integrated infrared intensity of the C–H stretch, the length of the gradient component along the C–X bond could be calculated and its behaviour in the series investigated. Unfortunately, no systematic study of the absolute intensities of the C–H stretches in these molecules has yet been made, so this polarizability hypothesis cannot be put to the test.

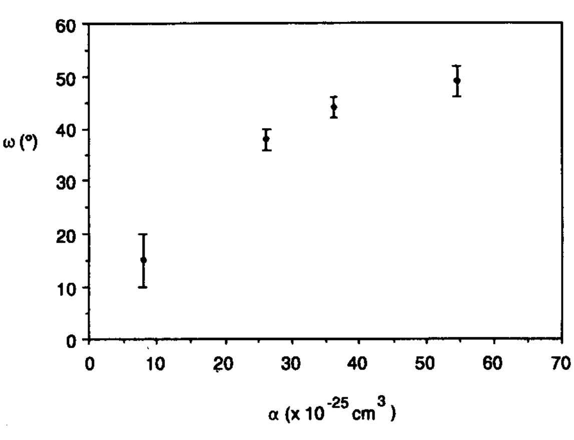

Fig. 11. The gradient angle ω for the partially deuterated methyl halides CHD_2X as a function of the polarizabilities α of the HX molecules.

Acknowledgements

The N.F.W.O. (Belgium) is thanked for a grant to one of us (A.Y.G.) and for financial support towards the spectroscopic equipment used in this study. The British Council is thanked for a travel grant. Professors Dr. W. Thiel and Dr. W. Schneider (Bergische Universität-Gesamthochschule, Wuppertal) are thanked for supplying the vibration–rotation interaction constants α_r^B for the partially deuterated methyl halides.

References

1 D.C. McKean, J. Mol. Struct., 113 (1984) 251.
2 B.J. van der Veken, R.O. Odeurs, A. Brown, D.C. McKean and A.R. Morrisson, J. Mol. Struct., 147 (1986) 57.
3 B.J. van der Veken, M.A. Herman and D.C. McKean, J. Mol. Struct., 114 (1984) 27.

4 F. Daeyaert, H.O. Desseyn and D.C. McKean, Spectrochim. Acta, Part A, 44 (1988) 1165.

5 F. Daeyaert and B.J. van der Veken, J. Mol. Struct., 198 (1989) 239.

6 A.Y. Grupping, D.C. McKean and B.J. van der Veken, J. Mol. Struct., 295 (1993) 273.

7 J.H. Newton and W.B. Person, J. Chem. Phys., 64 (1976) 3036.

8 A. Kindness, D.C. McKean and D. Stewart, J. Mol. Struct., 224 (1990) 363.

9 J.L. Duncan, J. Mol. Spectrosc., 60 (1976) 225.

10 W. Thiel and W. Schneider, personal communication, 1990.

11 P. Jensen, S. Brodersen and G. Guelachvili, J. Mol. Spectrosc., 88 (1981) 378.

12 R.F. Curl, Jr., J. Comput. Phys., 6 (1970) 367.

13 I.M. Mills and A.G. Robiette, Mol. Phys., 56 (1985) 743.

14 J.E. Baggott, D.A. Newnham, J.L. Duncan, D.C. McKean and A. Brown, Mol. Phys., 70 (1990) 715.

15 W.B. Person and J.H. Newton, J. Chem. Phys., 61 (1974) 1040.

16 S. Ilieva, T. Dudev and B. Galabov, Croat. Chem. Acta, 63 (1990) 143.

17 J.L. Duncan, Croat. Chem. Acta, 61 (1988) 463.

18 W. Schneider and W. Thiel, J. Chem. Phys., 86 (1987) 923.

19 M.D. Harmony, V.W. Laurie, R.L. Kuczkowski, R.H. Schwendemann, D.A. Ramsay, F.J. Lovas, W.J. Lafferty and A.G. Maki, J. Phys. Chem. Ref. Data, 8 (1979) 619.

20 Landolt-Börnstein, I. Band (Atom- und Molecularphysik), 3. Teil (Molekeln II), Springer-Verlag, Berlin, 1951.